Full-potential photoemission calculations for the Si(100) surface

1995 J. Phys.: Condens. Matter 7 7775

(http://iopscience.iop.org/0953-8984/7/40/008)

J. Phys.: Condens. Matter 7 (1995) 7775–7780. Printed in the UK

Full-potential photoemission calculations for the Si(100) surface

M Graß†, J Braun†, G Borstel† and S Bei der Kellen‡

† Department of Physics, University of Osnabrück, D-49069 Osnabrück, Germany

‡ Department of Physics and Astronomy, Northwestern University, Evanston, Il 60208-3112, USA

Received 21 June 1995

Abstract. In this contribution, we have calculated angle-dependent photoelectron spectra from the Si(100) surface along the ΓXWK bulk mirror plane by excitation with unpolarized He-I radiation. For this theoretical investigation the full-potential photoemission theory has been used, which is a straightforward generalization of the one-step model of photoemission in the case of anisotropic, space-filling cell potentials. The crystal potential employed for the determination of the theoretical data has been calculated self-consistently within the full-potential Korringa–Kohn–Rostoker band structure method. The comparison with the corresponding experimental data shows a very good agreement for all bulk transitions.

1. Introduction

Due to its great technical importance, the electronic structure of silicon has been subject to many investigations. Although various photoemission experiments have been carried out in order to determine the volume and surface band structure of silicon [1, 2, 3, 4, 5, 6], no comparative studies between calculated and measured angle-resolved ultraviolet photoemission intensities have been performed in the past. This can be understood as a consequence of the muffin-tin approximation which serves as the standard potential model in calculating angle-resolved ultraviolet photoemission (ARUPS) and bremsstrahlung isochromat spectra (ARBIS) within the original one-step theory of photoemission [7, 8]. For close-packed systems this potential model has been very successful [9, 10, 11, 12, 13], but for the treatment of solids with strong covalent bonding and open structure it provides only a rough approximation for the crystal potential. Consequently, the extension of the one-step model of photoemission to generally shaped cell potentials that leave no interstitial volume [14, 15, 16] enables us to calculate ARUPS spectra from the silicon (100) surface. The full-potential photoemission theory is directly based on the full-potential Korringa–Kohn–Rostoker (FP-KKR) method and makes use of all advantages of this modern band structure technique [17, 18, 19]. Moreover, it still contains all features of the fully dynamical one-step model.

In contrast to the (100) (2×1) surface of silicon, which has been observed in the experiment, for the calculated spectra no reconstruction effects have been taken into account, since a pure bulk potential is employed [19]. A theoretical study of surface-induced effects would require a full-potential slab calculation with the well known asymmetric dimer reconstruction. The result of such a calculation is a layer-dependent space-filling potential taking into account reconstruction and relaxation. Since no such calculation has

0953-8984/95/407775+06$19.50

been performed up to now, we employ the self-consistent FP-KKR bulk potential for all layers of the silicon crystal. Therefore, we expect a good agreement only for the bulk transitions. In the present paper, the general full-potential photoemission theory is briefly discussed in the following section 2. The relevant band structure for Si calculated self-consistently employing space-filling cell potentials is presented in section 3. Section 4 contains the calculated ARUPS spectra for the ΓXWK bulk mirror plane of the Si(100) surface. In order to compare the theoretical results with the measured data, we have used the parameters of the experimental configuration [2]. Section 5 contains a short summary.

2. Full-potential photoemission theory

The full-potential photoemission theory is based on the one-step model of photoemission and therefore describes the process of excitation and transport of the photo-emitted electrons in a fully dynamical way. The intensity of the photocurrent I as a function of the energy ϵ_f and the momentum of the photoelectron parallel to the surface $k_{||}$ can be written as

$$I(k_{||}, \epsilon_f) = -\frac{1}{\pi} \Im \left\langle k_{||}, \epsilon_f \middle| G_2^+ \; \Delta \; G_1^+ \; \Delta^* \; G_2^- \middle| \epsilon_f, k_{||} \right\rangle \tag{1}$$

at which the initial and final states of photoemission are represented by the propagators G_1^+ and $G_2^{\pm}$ respectively. The superscripts + (−) on the Green functions indicate forward (backward) propagation and the subscripts 1 (2) correspond to the energies of the initial (final) state wave field. Within the full-potential photoemission theory the photon field operator Δ describes the excitation process for an arbitrary shaped cell potential. The way in which this dipole operator is made accessible to practical calculations is described elsewhere [14, 15, 16]. In calculating the propagators G_1^+ and $G_2^{\pm}$ from full-potential multiple-scattering theory, we have to decompose the crystal with several atoms per unit cell into a semi-infinite stack of layers parallel to the surface. Each layer is built up with atomic cells of arbitrary shape, filled with the non-spherical crystal potential. These cells are centered at the atomic positions and leave no interstitial volume. It should be noted that one of the key quantities, namely the scattering matrix for a single layer, can also be used to calculate the band structure of the crystal under consideration. This procedure gives a check of the quality of the anisotropic, space-filling potential in use.

Within the one-step theory, the surface potential is considered as a one-dimensional barrier of the Rundgren–Malmström type [20, 21, 22], which has the height of the inner potential V_{0r}. The inner potential itself is estimated by the sum of the Fermi energy E_F and the work function W_F, which has been determined in the experiment as $W_F = 4.8$ eV [2]. Furthermore, in the framework of these calculations possible damping processes are taken into account in a phenomenological way, by adding an imaginary part V_{0i} to the inner potential of the crystal. V_{0i2} has been taken to be 2.0 eV for the final state. For the initial state wave field we have chosen $V_{0i1} = 0.05$ eV at Fermi energy, increasing to higher binding energies as $V_{0i1} = (0.05 - 0.01(E - E_F))$ eV. For the convergence of the angle-resolved intensities the number of reciprocal lattice vectors and the number of layers contributing to the photocurrent were carefully checked.

3. The crystal potential

The diamond structure of Si is an FCC lattice with a two-atom basis. These atoms are located at the points $(0, 0, 0)$ and $(\frac{1}{4}, \frac{1}{4}, \frac{1}{4})$. The anisotropic, space-filling potential representing the

ground state properties of the crystal has been calculated within the self-consistent FP-KKR band structure method [19]. In the framework of this theory, the crystal potential is decomposed into so-called atomic cells that contain one basis atom. The atomic cells are surrounded by bounding spheres and the potential inside each bounding sphere is expended in spherical harmonics:

$$V(r) = \sum_{lm} V_{lm}(r) Y_l^m(\hat{r}). \tag{2}$$

Each atomic cell has the full point group symmetry of the corresponding lattice point. Therefore, only the symmetry-adapted spherical harmonics are used in the above expansion [23]. To keep the maximum value l_{max} small, two additional empty cells have been introduced at the points $(\frac{1}{2}, 0, 0)$ and $(\frac{3}{4}, \frac{1}{4}, \frac{1}{4})$. These virtual cells guarantee a maximum value of $l_{max} = 4$ to be sufficient in describing the crystal potential. Fortunately, the empty cells have the same point group symmetry as the atomic cells. The non-spherical components of the cell potentials for an atomic and an empty cell can be found in figure 1. The strong variation of the components between the radius of the muffin-tin sphere and the bounding sphere ensure that the crystal potential is non-zero only inside the atomic cells. Moreover, the potential is almost spherically symmetric near the origin. A detailed analysis of this potential and the corresponding band structure can be found in [19]. As a first check of the quality of the potential in use we have reproduced the relevant band structure of Si along the Δ-direction in the Brillouin zone (see figure 2). This result has been obtained within the full-potential layer KKR technique of our photoemission code. It shows an excellent agreement with the original calculation of Bei der Kellen *et al* [19].

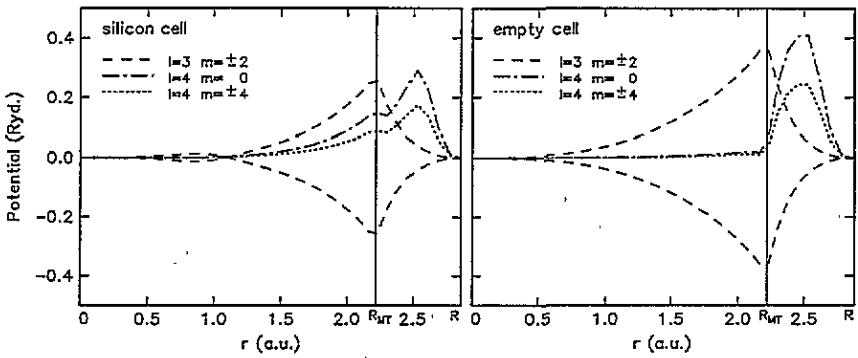

Figure 1. Non-spherical components of the self-consistent FP-KKR potential of silicon: the components for a silicon cell are shown in the left panel and the components for an empty cell in the right panel. The maximum value for the expansion in spherical harmonics is $l_{max} = 4$. R_{MT} is the radius of the muffin-tin sphere and R the radius of the bounding sphere.

As is common, density functional theory within the local density approximation (LDA) underestimates the optical gap. Therefore, the indirect band gap between $\Gamma_{25'}$ and 0.85 X is calculated to be $E_g = 0.49$ eV in contrast to the measured value of $E_g = 1.17$ eV [24]. In the calculation of the photocurrent the gap error has been corrected by renormalizing the excitation energy. This procedure is a well justified approximation for s–p-bonded systems since calculations within the GW approximation, which reproduce the band gap in good agreement with the experimental value, essentially show a rigid shift and only weak distortions in the conduction bands [25]. Finally, it should be noted that direct comparison of the calculated spectra with the experimental photoemission data enables us to determine the quality of the potential employed.

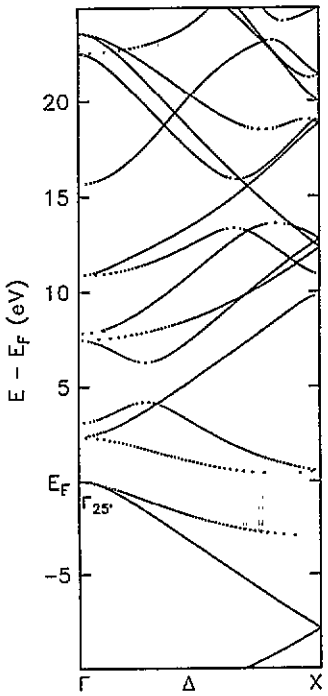

Figure 2. Calculated band structure of Si along the Δ-direction employing a self-consistent FP-KKR potential. The Fermi energy E_F represents the highest occupied state.

4. Results and discussion

The angle-resolved photoelectron intensities from the Si(100) surface calculated by excitation with unpolarized He-I radiation ($\hbar\omega = 21.2$ eV) are presented in this section. All spectra have been obtained by keeping the polar angle between the photon beam and and detected electrons constant at 40°. To take into account the experimental resolution, we have convoluted the calculated raw spectra with a Gaussian of 0.20 eV full width at half maximum.

The measured ARUPS data for the ΓXWK plane [2] and the corresponding full-potential photoemission calculations are shown in figure 3. For the whole range of emission angles $18° \leqslant \Theta \leqslant 42°$ six different bulk transitions and three surface states are visible. The intensities of these peaks are shown as a function of the initial state energy relative to the Fermi energy. The corresponding dispersions of all measured and calculated peaks are shown in figure 4 as a function of the wave vector parallel to the surface $k_{\|}$. It should be mentioned that the theoretical data have been taken from the raw spectra in order to determine the dispersions as exactly as possible.

From the figures 3 and 4 it can be seen that all calculated bulk transitions (labelled with a B) show very good agreement with the experimental data. All dispersive features have been reproduced within the experimental resolution. Only slight discrepancies of the relative intensities are visible and therefore the shoulder above B_{10} and the small peak B_9 with weak intensity cannot be clearly reproduced in the calculations. This might be due to the spherical averaging of the matrix elements. In contrast, the surface-induced peaks (labelled with an S) are not in accordance with the calculations. As a consequence of the bulk character of the potential used in our the calculations the surface state S_1 shows an

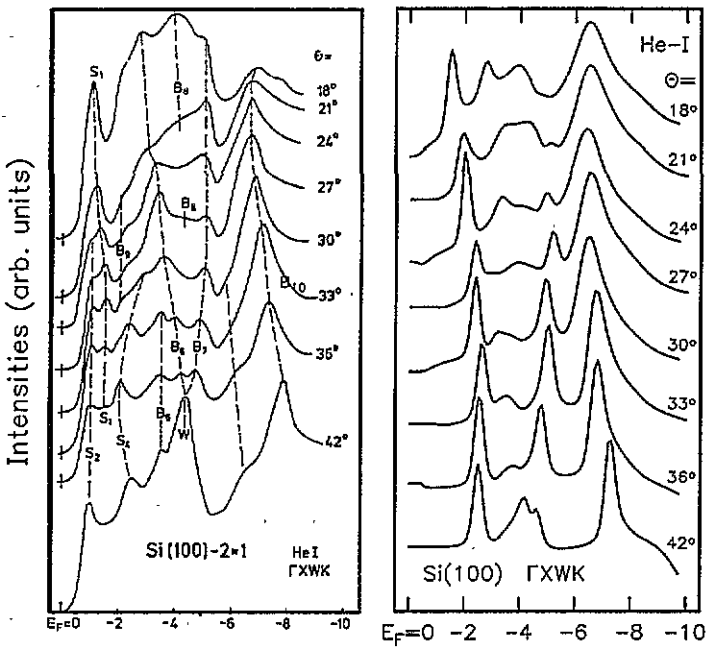

Figure 3. Comparison of measured [2] (left panel) and calculated (right panel) angle-resolved valence band spectra for the Si(100) surface in the ΓXWK emission plane using unpolarized He-I (21.2 eV) radiation.

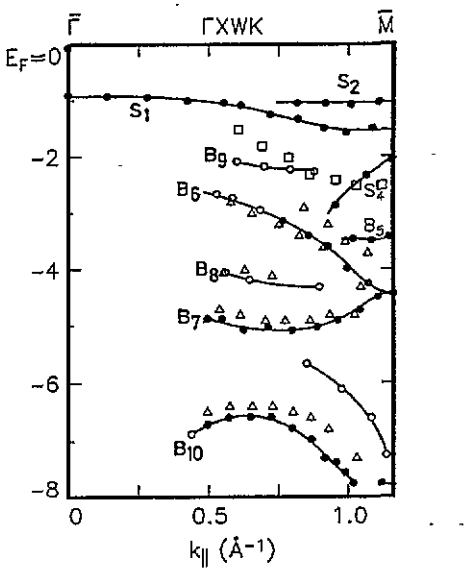

Figure 4. Dispersion of initial state energies of peaks observed in figure 3 versus $k_{||}$. The peaks with weak (strong) intensities observed in the experiment are marked with open (solid) circles. The open triangles (squares) denote calculated transitions from bulk (surface) states.

incorrect dispersion. Moreover, the neglecting of surface-induced effects on the pure bulk potential leads to the absence of the surface states S_2 and S_4 in the calculations.

The employment of a self-consistent layer-dependent FP-KKR potential should be able

to overcome these discrepancies.

In conclusion, we can state that the full-potential photoemission theory enables us to calculate photoelectron intensities from bulk states of systems with open structures like silicon in quantitative agreement with measured data. We are currently working on the computational implementation of the fully relativistic full-potential photoemission theory and we are looking forward to presenting further results.

Acknowledgment

Financial support of this work by the Deutsche Forschungsgemeinschaft is gratefully acknowledged.

References

[1] Koke P, Goldmann A, Mönch W, Wolfgarten G and Pollmann J 1985 *Surf. Sci.* **152/153** 1001
[2] Goldmann A, Koke P, Mönch W, Wolfgarten G and Pollmann J 1986 *Surf. Sci.* **169** 438
[3] Johansson L S O, Uhrberg R I G and Hansson G V 1987 *Surf. Sci.* **189/190** 479
[4] Johansson L S O, Persson P E S, Karlsson U O and Uhrberg R I G 1990 *Phys. Rev.* B **42** 8991
[5] Schmiedeskamp B, Vogt B and Heinzmann U 1990 *Solid State Commun.* **76** 1391
[6] Cho J and Nemanich R J 1992 *Phys. Rev.* B **46** 15 212
[7] Pendry J B 1976 *Surf. Sci.* **57** 679
[8] Hopkinson J F L, Pendry J B and Titterington D J 1980 *Comput. Phys. Commun.* **19** 69
[9] Larsson C G 1985 *Surf. Sci.* **152/153** 213
[10] Lindroos M, Hofmann P and Menzel D 1986 *Phys. Rev.* B **33** 6798
[11] Ginatempo B and Gyorffy B L 1990 *J. Phys.: Condens. Matter* **2** 5233
[12] Schneider R, Starke K, Ertl K, Donath M, Dose V, Braun J, Graß M and Borstel G 1992 *J. Phys.: Condens. Matter* **4** 4293
[13] Braun J and Borstel G 1993 *Phys. Rev.* B **48** 14373
[14] Graß M, Braun J and Borstel G 1993 *Phys. Rev.* B **47** 15 487
[15] Graß M, Braun J and Borstel G 1994 *Prog. Surf. Sci.* **46** 107
[16] Graß M, Braun J and Borstel G 1994 *Phys. Rev.* B **50** 14 827
[17] Brown R G and Ciftan M 1986 *Phys. Rev.* B **33** 7937
[18] Butler W H, Gonis A and Zhang X-G 1992 *Phys. Rev.* B **45** 11 527
[19] Bei der Kellen S, Oh Y, Badralexe E and Freeman A J 1995 *Phys. Rev.* B **51** 9560
[20] Malmström G and Rundgren J 1980 *Comput. Phys. Commun.* **19** 263
[21] Rundgren J and Malmström G 1977 *J. Phys. C: Solid State Phys.* **10** 4671
[22] M. Graß Braun J, Borstel G, Schneider R, Dürr H, Fauster Th and Dose V 1993 *J. Phys.: Condens. Matter* **5** 599
[23] Altmann S L and Cracknell A P 1965 *Rev. Mod. Phys.* **37** 19
[24] 1987 Semiconductors: intrinsic properties of group elements and III–V, II–VI and I–VII compounds *Landolt–Börnstein New Series* Group III, vol 22a (Berlin: Springer)
[25] Rohlfing M, Krüger P and Pollmann J 1993 *Phys. Rev.* B **48** 17 791